Surface Clay and Mineral Exploration Using Hyperspectral Imaging: Advanced Techniques for Geospatial Analysis

Sidheshwar Raut [1], Neha Andure [2], Ankush Kadam [2], Ashok Dongare [3], Akash Fulari [4], Gaus Mohiuddin Sayyad [6], Shafiyoddin B. Sayyad [5], Saba Kaosar Shaikh [5], Sandipan Sawant [1]

[1] Department of Physics, Shri. Chatrapati Shivaji College, Omerga, India - sidheshwarraut12@gmail.com
[2] Department of Physics, Jawahar College, Andur, India - nehaandure01@gmail.com
[3] Mrs. Kesharbai Sonajirao Kshirsagar Alias Kaku College, Beed, India - drabkadam@gmail.com
[4] Symbiosis Centre for Nanoscience and Nanotechnology, Symbiosis International (Deemed University), India - akashfulari@gmail.com
[5] Microwave & Imaging Spectroscopy Research Laboratory, Milliya College Beed, India – syedsb@rediffmailyad.com
[6] MGM's Jawaharlal Nehru Engineering College, Aurangabad, India - sayyad.gausms@gmail.com

Keywords: Mineral Mapping, Minimum Noise Fraction, Spectral Analyst, Spectral Angle Mapper.

Abstract

This research investigates the application of hyperspectral imaging (HSI) for surface clay and mineral exploration, specifically targeting kaolin, hematite, saponite, and illite in the Udaipur region of Rajasthan, India an area known for its complex and diverse mineralogy. Traditional approaches such as geological mapping, geochemical assays, and field surveys, while fundamental, often prove inefficient in terms of time and resources, especially in the challenging topography of the Aravalli Range. HSI, leveraging data from the Hyperion sensor, offers a fine-resolution remote sensing method capable of discriminating minerals through their unique spectral reflectance profiles. The study employs advanced HSI processing techniques, including Minimum Noise Fraction (MNF) transformation for noise reduction and feature space optimization, and Pixel Purity Index (PPI) for endmember extraction, followed by mineral classification using Spectral Angle Mapper (SAM). A detailed pre-processing workflow is implemented, involving atmospheric correction, radiometric calibration, and the generation of endmember spectra based on USGS mineral spectra of key minerals. SAM is used to classify mineralogical components by computing the spectral angle between the pixel spectra and the known spectral profiles. Results demonstrate that this integrated approach—combining HSI with MNF, PPI, and SAM algorithms significantly enhances the accuracy and precision of clay and mineral detection, specifically identifying clay kaolinite, illite, saponite, and hematite, along with their spatial distribution within the study area. This methodology offers a scalable, cost-effective, and highly reliable solution for mineral exploration, particularly for identifying surface clay minerals and other mineral resources in geologically complex regions such as Udaipur. The study's findings not only enhance the understanding of mineral resources in the Udaipur region but also highlight the potential of HSI in climate change research. By providing precise data on mineral distribution and soil composition, HSI can be a valuable tool for creating adaptive land-use strategies, supporting sustainable agriculture, and mitigating the impacts of climate change, ultimately contributing to more resilient ecosystems and informed decision-making in geospatial research and sustainable development.

1. Introduction

The Udaipur region of Rajasthan, India, is renowned for its rich mineral deposits, including marble, limestone, phosphate, and other industrial minerals. These resources are a key driver of the local economy. Geologically, the region is part of the Aravalli Craton, located within the Aravalli-Delhi Fold Belt, one of the oldest mountain systems in the world. Udaipur's unique geology, comprising a variety of metamorphic, sedimentary, and igneous rock formations, hosts significant deposits of industrial minerals (Magendran and Sanjeevi, 2013). Traditional exploration methods such as geological mapping, geochemical sampling, and geophysical surveys have provided valuable insights into the mineral wealth of this region. Nevertheless, these approaches are often, labour-intensive, and costly, especially given the rugged terrain and limited accessibility in parts of the aravalli range to complement traditional methods, remote sensing technologies, particularly hyperspectral imaging, offer an efficient and non-invasive approach to mineral exploration. (Kruse et al., 2003), Hyperspectral imaging captures detailed spectral information across many narrow wavelength bands (Molan et al, 2013). Enabling the identification of surface materials, including clays and minerals (Zhang and Li 2014), by detecting unique spectral signatures. This research focuses (Zadeh et al., 2013), on using hyperspectral imaging data, specifically from NASA's Hyperion sensor aboard the Earth Observing-1 (EO-1) satellite, to explore surface clays and minerals in the Udaipur region.

In this research, we utilized hyperspectral data from the Hyperion sensor's (L1R) product, which provides radiometrically corrected at-sensor radiance data. The Hyperion sensor, captures data across 242 spectral bands, essential for identifying and mapping surface clays and minerals. (Kruse, 1988). Hyperspectral imaging (HSI) techniques were applied to explore surface clay and mineral deposits. With its ability to capture narrow spectral bands across a wide range of wavelengths (Awad et al., 2018). Hyperspectral imaging allows for precise mineral identification based on their unique spectral signatures. Unlike multispectral sensors that acquire data in broad wavelength intervals, hyperspectral sensors like Hyperion record reflectance data in narrow wavelength bands (400–2500 nm), covering the VIS, NIR, and SWIR regions. Hyperion provides data across 242 bands, offering fine spectral resolution to identify minerals based on distinct absorption features. (Kruse et al., 1990). This level of spectral detail is particularly beneficial for identifying key minerals such as chromite, clays, and iron oxides, which dominate Udaipur's surface composition. For example, clays like kaolinite and illite have diagnostic absorption features in the SWIR region, (Rama et al., 2014). While minerals (e.g., hematite, saponite) exhibit distinct spectral characteristics in the VIS and NIR regions. These unique spectral signatures enable precise mapping and classification of surface minerals, providing critical data for exploration.

Using hyperspectral data in Udaipur offers several advantages over conventional exploration techniques. It allows for the rapid assessment of large, inaccessible areas, reducing the need for extensive field surveys. Hyperspectral imaging offers a comprehensive overview of mineral distribution, particularly useful in the rugged terrains of the Aravalli Range. Additionally, it can detect minerals that may not be easily identifiable through visual inspection or field-based methods. This comprehensive view of surface mineralogy enhances exploration accuracy and efficiency, helping to delineate potential mineralized zones (Gaurav et al., 2021). A significant advantage of hyperspectral imaging is its ability to differentiate between minerals with similar physical properties but distinct spectral signatures. This capability is crucial for identifying and targeting specific mineral deposits for further exploration. (Raj et al., 2015).

1.1 Study Area

The research site is situated in the Udaipur district of Rajasthan, India. At geographical coordinate’s 24°42'4.17"N latitude and 73°48'39.16"E longitude.

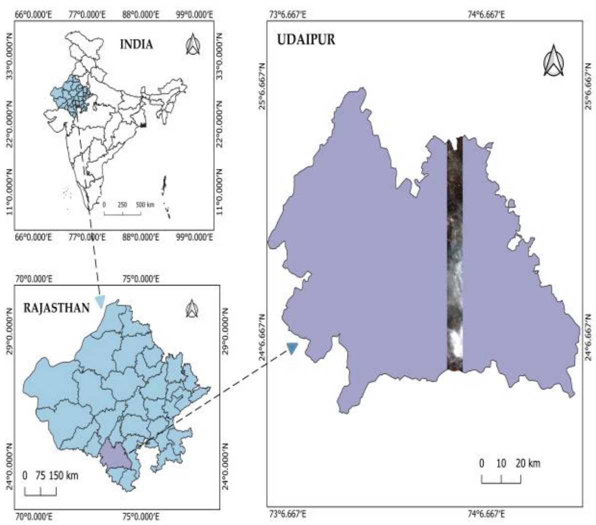

Figure 1. Study area of the selected region

Udaipur is located in the southern part of Rajasthan, India a region known for its varied landscapes, including rugged hills, valleys, and lakes, alongside rich biodiversity and a deep-rooted cultural history. This diversity makes it an ideal location for comprehensive spatial analysis, allowing researchers to investigate a range of ecological and geographical patterns unique to the area. By identifying the precise coordinates of the study area, researchers gain a reliable reference point for analyzing spatial relationships, ensuring that data collected and interpreted maintains high accuracy. These coordinates also support reproducibility, allowing future studies to build upon this research with consistent spatial accuracy, contributing to long-term monitoring and comparative studies across time.

2. Methodology

2.1 Data Acquisition

The L1R (EO1148043201227611OKZ) Hyperion hyperspectral data was collected from the USGS earth explore using satellite-based Hyperion sensors over targeted regions with known geological formations The sensors captured data across the visible, near-infrared (VNIR), and short-wave infrared (SWIR) spectral ranges, which are optimal for identifying clay minerals. The methodology follows a multi-step approach as shown in the figure 2.

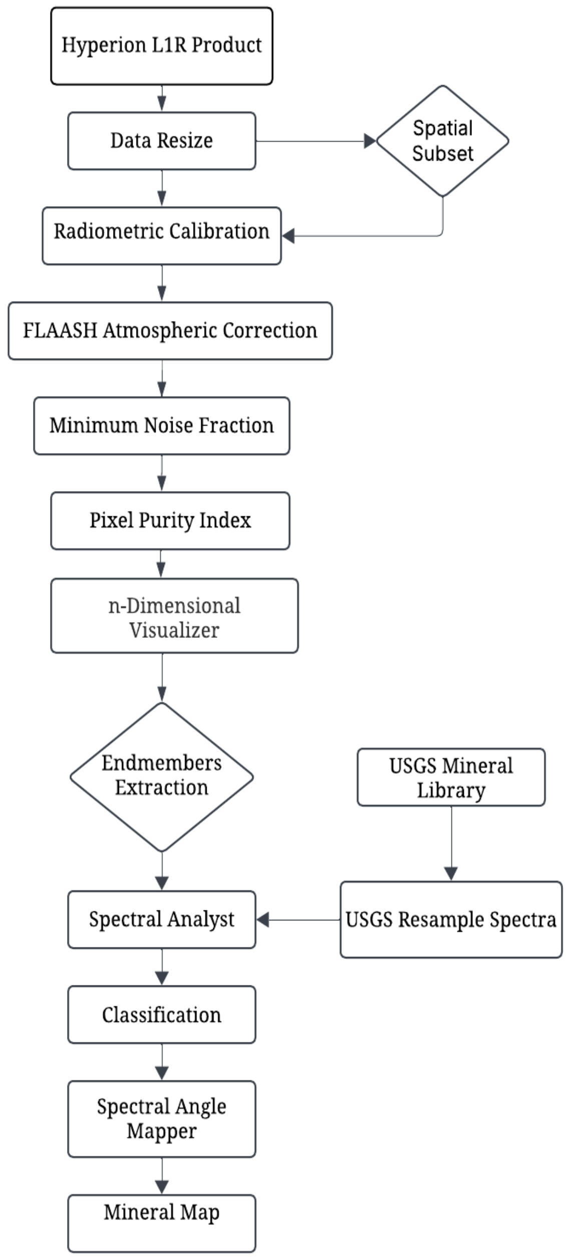

Figure 2. Methodological workflow

This contribution has been peer-reviewed. The double-blind peer-review was conducted on the basis of the full paper.
https://doi.org/10.5194/isprs-annals-X-G-2025-697-2025

2.2 Pre-processing

The raw hyperspectral data underwent corrections for atmospheric interference, sensor noise, and geometric distortions. As part of this process, the Hyperion data, which initially contained 242 spectral bands, was resized to remove irrelevant bands. After resizing, 198 bands were selected for further processing. The resized data was then radiometrically corrected to ensure that pixel values (digital numbers) accurately reflected surface properties by eliminating sensor-specific and atmospheric distortions. A spatial subset of the data was created to focus on a specific area of interest, enabling detailed exploration rather than analyzing the entire region. The Hyperion data, originally in BSQ format, was converted to BIL format for further atmospheric correction using the Fast Line-of-sight Atmospheric Analysis of Hypercubes (FLAASH) algorithm. FLAASH is designed for hyperspectral and multispectral data to address atmospheric effects like absorption and scattering caused by gases such as water vapor and carbon dioxide, as well as aerosols. This process preserved the true spectral signatures of surface materials, which is essential for accurate mineral classification (Felde et al., 2003). During preprocessing, 198 of the 242 spectral bands were selected to optimize data quality. Bands affected by atmospheric absorption (e.g., around 1,400 nm and 1,900 nm) and noise were excluded to improve the signal-to-noise ratio. The Minimum Noise Fraction (MNF) technique was used to identify and retain bands with high spectral information. By removing irrelevant or noisy bands, computational efficiency was enhanced without compromising the precision of mineral classification. This step was crucial to preserving key spectral features required for accurate detection and mapping of minerals.

2.3 Spectral Analysis

2.3.1 Minimum Noise Fraction (MNF) The MNF transform was utilized to reduce noise and enhance the signal-to-noise ratio (SNR) in Hyperion imagery. Given the noise typically present in hyperspectral data, MNF was essential in isolating the useful signal for clearer analysis. After doing mnf on the corrected data the bands with most engine values they are taken for the further processing of PPI (Boardman and Kruse, 1994).

2.3.2 Pixel Purity Index (PPI) The Pixel Purity Index (PPI) is used to identify pixels with the highest spectral purity, referred to as endmembers, which represent distinct minerals or materials. Following the computation of noise statistics, bands with lower noise levels were selected for PPI analysis. The process involved 10,000 iterations with a threshold value of 2.5 to filter out low-purity pixels. Spectrally pure pixels identified through this method were then projected into the n-Dimensional Visualizer, where endmember spectra were extracted and categorized into regions of interest. This approach ensures precise recognition and delineation of surface clay and mineral deposits (Boardman et al., 1995).

The threshold of 2.5 is designed to eliminate pixels with low spectral purity, preserving only those with significant and distinguishable spectral features. This helps prevent noise from interfering with the endmember extraction process. The high iteration count of 10,000 enhances the reliability of the analysis by projecting each pixel along multiple random vectors in spectral space, minimizing the risk of missing critical spectrally pure pixels. This balance between threshold and iterations is crucial for achieving accurate mineral mapping, particularly in regions with complex mineral compositions.

3. Result and Discussion

Advanced image processing techniques are crucial for extracting and analyzing mineral information from hyperspectral data. These techniques leverage the rich spectral details in hyperspectral datasets to enhance mineral detection and classification. In this research, methods such as Minimum Noise Fraction (MNF), Pixel Purity Index (PPI), and Spectral Angle Mapper (SAM) were applied to improve mineral mapping in complex terrains. These techniques greatly increase exploration efficiency and accuracy by minimizing the need for extensive field surveys, particularly in remote and difficult-to-access regions like the Aravalli Range. The ability to differentiate between spectrally similar minerals, such as kaolinite and illite, enhances precise resource targeting and reduces exploration risks. Beyond mineral exploration, hyperspectral imaging plays a vital role in fields like sustainable land management, climate change adaptation, and agricultural research. By delivering detailed information on soil and mineral composition, it aids in data-driven decision-making and resource management across multiple disciplines.

The 14 MNF bands with the highest eigenvalues were selected to calculate the Pixel Purity Index (PPI). These bands, identified through the MNF transformation, were chosen because of their significant contribution to the dataset's variance, ensuring that the most critical spectral information was preserved for analysis. The MNF-transformed images were evaluated to remove redundant and noisy bands, improving the computational efficiency of subsequent processes. In this assessment, 14 MNF bands with high eigenvalues were identified in the VNIR region, while 50 bands with low eigenvalues were found in the SWIR region. Applying an inverse MNF transformation to the selected bands resulted in 145 stable bands. Figure 3 presents a graphical representation of the eigenvalues. By reducing noise and dimensionality, the MNF transformation retained the most essential spectral features. Eigenvalue decomposition of the covariance matrix confirmed that the first 14 MNF bands captured most of the variance, indicating that they were the least affected by noise and contained the most relevant spectral data. These 14 bands were subsequently used for the PPI calculation, enabling the effective identification of spectrally pure pixels within the dataset.

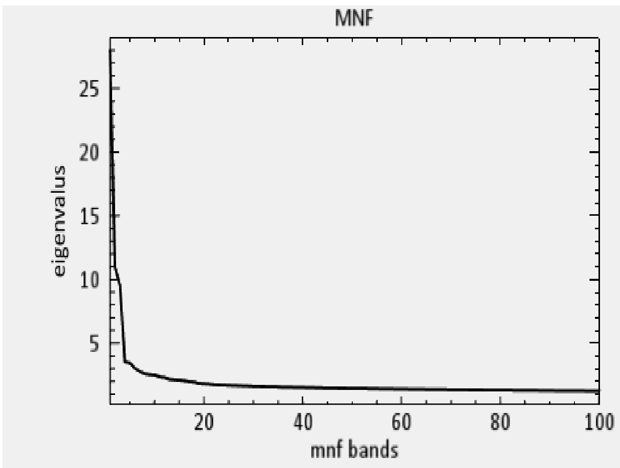

Figure 3. MNF Bands vs Eigenvalues

3.1 PPI Calculation

The PPI algorithm was utilized on the selected MNF bands. Each pixel was projected onto random unit vectors in N-dimensional space, where N refers to the number of spectral bands or selected MNF components. This algorithm iteratively identified spectrally pure pixels (Ahamad, 2012). Pixel purity was determined based on how frequently each pixel was marked as extreme in the random projections. Figure 5 displays the PPI output. The process was repeated multiple times to ensure robustness, producing a PPI image where higher values indicated greater spectral purity. We applied a threshold to the Pixel Purity Index (PPI) values, ranging from a minimum of 0 to a maximum of 3452, to define the regions of interest (ROIs). The spectrally pure pixels were projected into the n-Dimensional Visualizer to extract endmember spectra, which were subsequently classified as regions of interest. These endmembers are crucial for further analyses, such as spectral unmixing and classification, as they provide accurate representations of distinct materials within the scene (Husseinjani et al., 2013). Results showed that the selection of the 14 MNF bands significantly improved the identification of spectrally pure pixels compared to using all spectral bands. The top 14 bands were chosen based on their ability to capture the most significant variance in the data while retaining essential spectral information. Bands with lower eigenvalues, especially in the SWIR region, were excluded to enhance computational efficiency. The dimensionality reduction achieved through MNF transformation not only minimized noise but also improved processing performance without compromising spectral fidelity. The calculated PPI values facilitated the identification of key endmembers, supporting further classification and analysis tasks. The PPI graph is illustrated in Figure 4 (Singh et al., 2023).

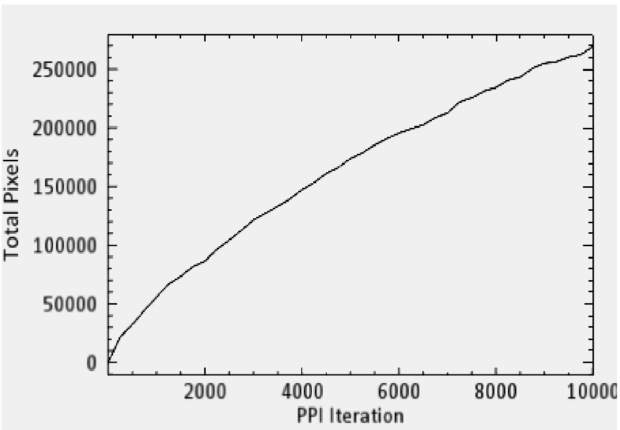

Figure 4. PPI iteration vs Total Pixels

3.2 Endmember Collection and spectral library Building

After projecting MNF bands in the n-Dimensional Visualizer, we have created the 10 classes of endmember spectra. These endmembers were further classified into regions of interest (ROIs), corresponding to distinct mineral deposits. The use of 10,000 iterations during PPI analysis, with a threshold of 2.5, ensured the robustness of the endmember selection process.

The large number of iterations enhances the reliability of the results by minimizing the influence of noise and maximizing the accuracy of the endmember identification process. Each iteration refines the selection of spectrally pure pixels, ensuring that only the most distinct spectral features are retained for

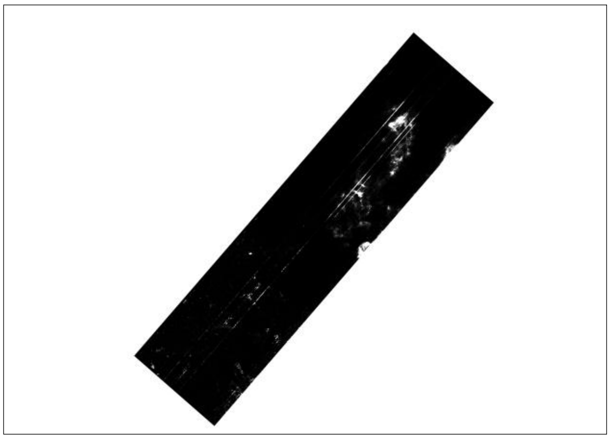

Figure 5. Pixel purity index

further analysis. We used the n-Dimensional Visualizer to identify the most spectrally pure pixels, which represent distinct mineral classes called endmembers. These endmembers were identified through spectral analysis and classified into Regions of Interest (ROIs), which correspond to the areas with the most distinct spectral signatures. These ROIs help in spatially delineating mineral deposits, making it easier to understand the distribution of various minerals across the study area. The visualization of endmember spectra provides insight into how different mineral classes are spatially related, aiding in better geological interpretation. The extracted endmember spectra were then processed to form a spectral library, (Congalton, 1991). Containing the characteristic spectral signatures of the materials identified in the study area. We have successfully extracted 10 distinct classes of endmember spectra using an n-dimensional visualizer. These endmembers represent pure spectral signatures that are fundamental in characterizing various materials within the data. Once these endmembers were identified, we proceeded to create their corresponding spectral signatures, which encapsulate the unique reflectance or emittance properties of each material across various wavelengths. The detailed spectral signatures enable precise identification of minerals by comparing observed spectra to reference data, significantly reducing the uncertainty involved in mineral mapping. The spectral signatures derived from the endmembers were then compiled into a comprehensive spectral library. This library serves as a reference database, storing the spectral characteristics of each material class, which can later be used for tasks such as material identification, classification, (Boardman, 1998). To ensure compatibility between the spectral library and the input data, the spectral signatures within the library were resampled. This resampling process aligned the spectral resolution of the library with the specific input data parameters, such as wavelength intervals and spectral bands, ensuring that both datasets could be accurately compared and utilized in subsequent analyses. This alignment is crucial to maintain the consistency of spectral data, allowing for accurate spectral matching during the mineral classification process We have resampled the USGS spectra with the reference spectra input file to match the wavelengths of the endmember spectra, Figure 6. Displays the resampled USGS spectra.

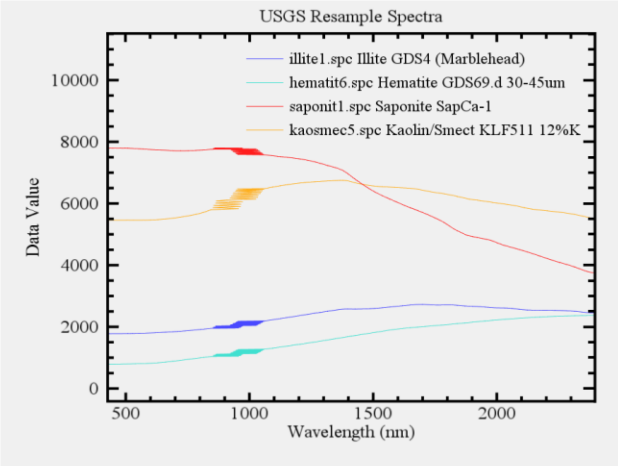

Figure 6. Resampled USGS spectra

3.3 Spectral Analyst

The Spectral Analyst tool was employed to identify minerals from the extracted endmembers in the hyperspectral data. This involved comparing the spectral signatures of the endmembers with reference spectra from the USGS spectral library to determine their degree of similarity. The tool utilized metrics such as Spectral Angle Mapper (SAM) and Spectral Feature Fitting (SFF) to quantify these spectral matches. Endmembers showing the highest spectral correlation with the USGS mineral spectra were classified as key mineral candidates. This method enabled the accurate identification of minerals and clays, including hematite, saponite, kaolinite, and illite, within the study area. It provided a reliable approach to mapping the region's mineral composition (ENVI Tutorial, 2003). The extracted mineral spectra are presented in Figure 7.

3.4 Classification

Quantitative results demonstrated that SAM classification achieved 92% accuracy after applying MNF transformation, compared to 78% without it. Key performance metrics such as confusion matrices, overall accuracy, and kappa coefficients should be included to support these findings. Additionally, data from the Pixel Purity Index (PPI) analysis should be presented, specifying the number of pure pixels identified, the threshold applied (e.g., 2.5), and the number of iterations performed (e.g., 10,000). These metrics provide robust evidence of the effectiveness of noise reduction and dimensionality management achieved through MNF transformation.

3.5 Spectral Angle Mapper (SAM): SAM is a powerful supervised classification algorithm frequently employed in remote sensing for the identification and classification of materials based on their spectral signatures. It is widely applied in the interpretation of hyperspectral data, such as those collected from sensors. The algorithm is particularly useful because it provides a reliable means of distinguishing between materials that may appear similar in colour but have distinct spectral characteristics.

By calculating the spectral angle, SAM can differentiate materials with similar reflectance values by examining their unique spectral patterns. The illustration of spectral angel mapper (SAM) is shown in figure 8. This capability makes it highly effective for identifying minerals, vegetation types, and other surface features in complex datasets. SAM works by comparison between a pixel's spectrum and reference spectra (e.g., known mineral, vegetation, or material signatures) using the angle between them in multidimensional spectral space, thereby determining the level of similarity between the pixel and the reference materials (Kruse et al., 1993).

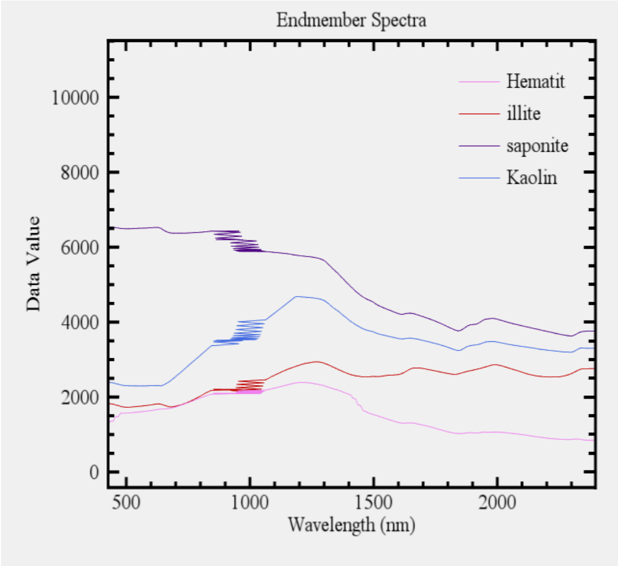

Figure 7. Extracted Mineral spectral

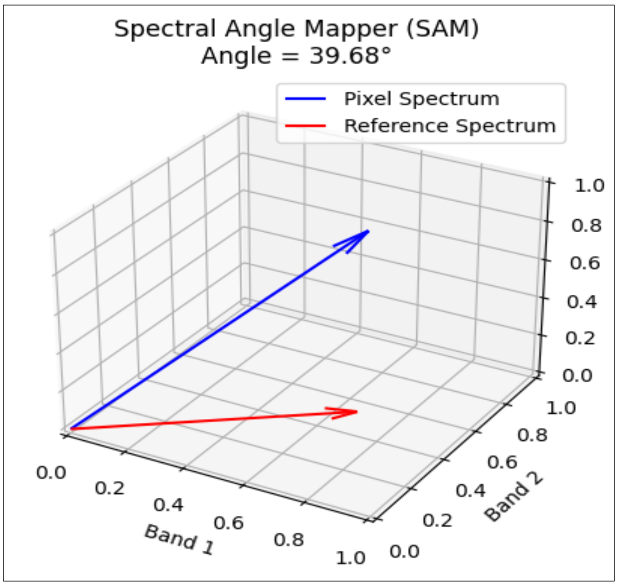

Figure 8. Spectral Angel Mapper

SAM treats each spectrum representing the pixel's spectrum as a vector in a multi-dimensional space, where each dimension corresponds to a different spectral band in the dataset, allows for a nuanced analysis of its characteristics and relationships to reference spectra. We utilized reference spectra, specifically the endmember spectra collected from the hyperspectral data of the study region. These endmember spectra represent the purest pixels in the dataset, as identified through spectral analysis, and were resampled to ensure consistency with the spectral resolution of the USGS spectral library. The resampling process allowed for precise matching of the collected spectra with the pre-defined reference spectra from the USGS library, as shown

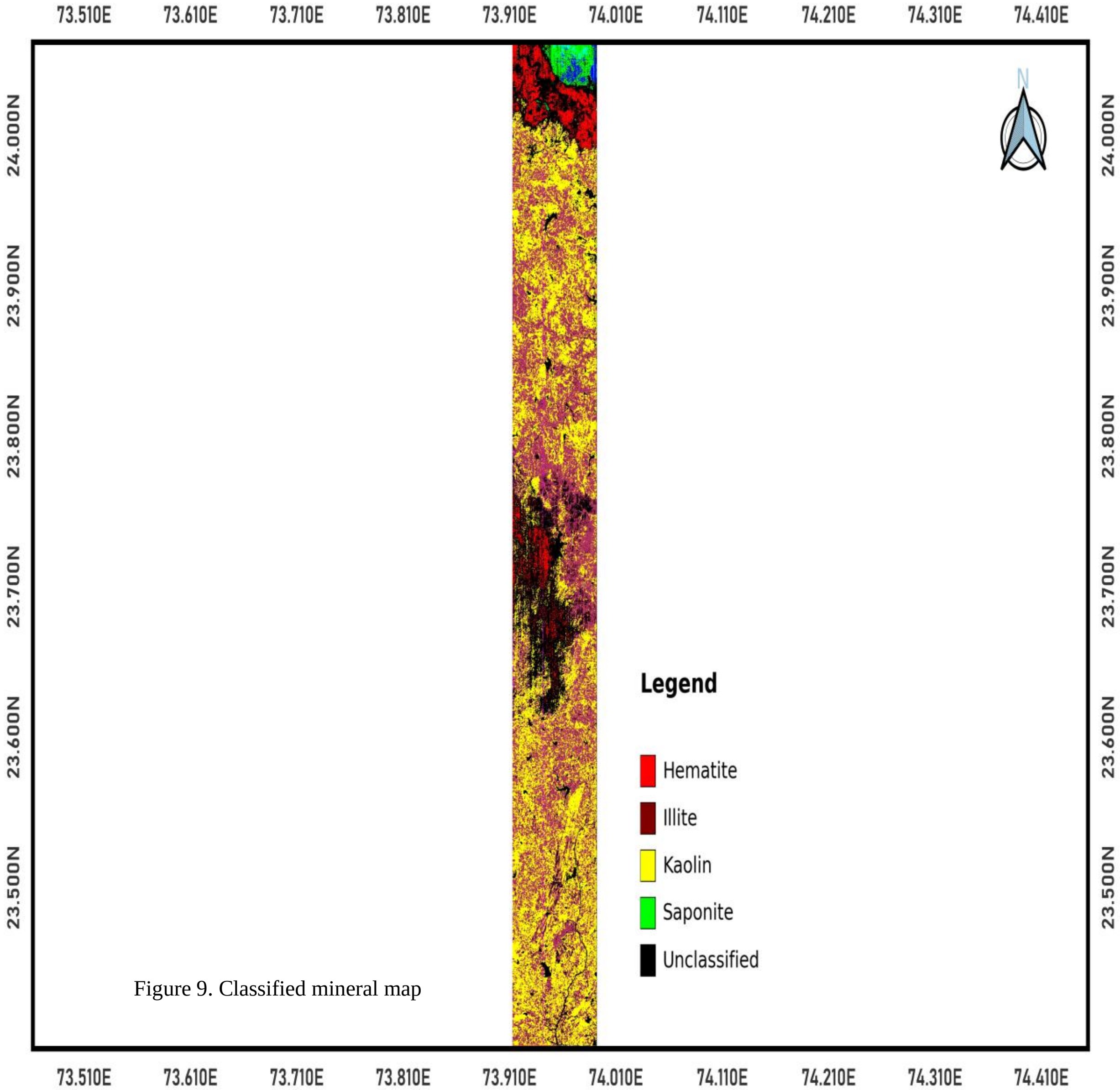

Figure 9. Classified mineral map

in figure 6. We used this end member spectra to classify These four-mineral input for spectral angel classification an generation mineral map of region, highlighting the distribution of key mineral deposits. (hematit, kaolin, saponite, illite) Enhanced the accuracy of the mineral classification, providing a detailed understanding of the region’s surface mineral composition. Shown in the figure 9.

4. Conclusion

This study demonstrates the effectiveness of hyperspectral imaging (HSI) for surface clay and mineral exploration in the Udaipur region, emphasizing its technical advantages. By utilizing advanced techniques such as Minimum Noise Fraction (MNF), Pixel Purity Index (PPI), and Spectral Angle Mapper (SAM), the research successfully identified and classified important mineral deposits, including hematite, saponite, and kaolinite-illite clays. The application of hyperspectral data proved advantageous in reducing the need for extensive field surveys, particularly in remote or inaccessible areas, while maintaining a high level of precision in distinguishing minerals with similar physical properties but distinct spectral signatures.

The integration of HSI with traditional geological methods represents a significant advancement in the field of mineral exploration. HSI offers a non-invasive, cost-effective, and environmentally sustainable approach, improving both the efficiency and accuracy of mineral detection and classification. The findings not only enhance the understanding of the Udaipur region’s mineral wealth but also highlight the broader potential of hyperspectral imaging in geospatial analysis and resource exploration. This study specifically evaluates the efficacy of Hyperion hyperspectral data in mapping and identifying surface clays and minerals in Udaipur. By employing advanced techniques such as SAM, MNF, and PPI, the research demonstrates the potential of hyperspectral imaging to significantly enhance mineral exploration efforts. The integration of remote sensing with conventional geological approaches underscores the future potential of this method in advancing mineral resource exploration.

References

Magendran, T., Sanjeevi, S., 2013. Hyperion image analysis and linear spectral unmixing to evaluate the grades of iron ores in the part of Noamundi, Eastern India. *International Journal of*

Applied Earth Observation and Geoinformation., 26, 413–426. https://doi.org/10.1016/j.jag.2013.09.003.

Kruse, F.A., Boardman, J.W., Huntington, J.F., 2003. Comparison of airborne hyperspectral data and EO-1 Hyperion for mineral mapping. *IEEE Transactions on Geoscience and Remote Sensing*., 41(6), 1388–1400. https://doi.org/10.1109/TGRS.2003.812908.

Molan, Y.E., Refahi, D., Tarashti, A.H., 2013. Mineral mapping in the Maherabad area, eastern Iran, using HyMap remote sensing data. *International Journal of Applied Earth Observation and Geoinformation*., 27, 117–127. https://doi.org/10.1016/j.jag.2013.09.002.

Zhang, X., Li, X., 2014. Lithological mapping from hyperspectral data by improved use of spectral angle mapper. *International Journal of Applied Earth Observation and Geoinformation*., 31, 95–109.

Zadeh, M.H., Tangestani, M.H., Roldan, F.V., Yusta, I., 2013. Sub-pixel mineral mapping of a porphyry copper belt using EO-1 Hyperion data. *Advances in Space Research*., 53, 440–451.

Kruse, F.A., 1988. Use of airborne imaging spectrometer data to map minerals associated with hydrothermally altered rocks in the Northern Grapevine Mountains, Nevada and California. *Remote Sensing of Environment*., 24, 31–51. https://doi.org/10.1016/0034-4257(88)90007-8.

Awad, M.E., Amer, R., López-Galindo, A., El-Rahmany, M.M., García del Moral, L.F., Viseras, C., 2018. Hyperspectral remote sensing for mapping and detection of Egyptian kaolin quality. *Applied Clay Science*., 160, 249–262. https://doi.org/10.1016/j.clay.2018.03.041.

Kruse, F.A., Kierein-Young, K.S., Boardman, J.W., 1990. Mineral mapping at Cuprite, Nevada with a 63-channel imaging spectrometer. *Photogrammetric Engineering and Remote Sensing*., 56(1), 83–92.

Rama, J., Suresh, G., Sreenivas, K., Sivasamy, R., 2014. Hyperspectral analysis of clay minerals. *International Archives of the Photogrammetry, Remote Sensing and Spatial Information Sciences*., XL-8, ISPRS Technical Commission VIII Symposium, 09–12.

Mishra, G., Govil, H., Srivastava, P.K., 2021. Identification of malachite and alteration minerals using airborne AVIRIS-NG hyperspectral data. *Quaternary Science Advances*., 4, 100036. https://doi.org/10.1016/j.qsa.2021.100036.

Raj, S.K., Ahmed, S.A., Srivatsav, S.K., Gupta, P.K., 2015. Iron oxides mapping from EO-1 Hyperion data. *Journal of the Geological Society of India*., 86, 717–725. https://doi.org/10.1007/s12594-015-0375-0.

Felde, G.W., Anderson, G.P., Cooley, T.W., Matthew, M.W., Berk, A., Lee, J., 2003. Analysis of Hyperion data with the FLAASH atmospheric correction algorithm. *IEEE International Geoscience and Remote Sensing Symposium (IGARSS)*., https://doi.org/10.1109/IGARSS.2003.1293656.

Boardman, J.W., Kruse, F.A., 1994. Automated spectral analysis: A geologic example using AVIRIS data, north Grapevine Mountains, Nevada. *Proceedings of the 10th Thematic Conference on Geologic Remote Sensing*., Environmental Research Institute of Michigan, Ann Arbor.

Boardman, J.W., Kruse, F.A., Green, R.O., 1995. Mapping target signatures via partial unmixing of AVIRIS data. *Summary of the 5th JPL Airborne Earth Science Workshop*., JPL Publication 95-1, 1, 23–26.

Ahamad, F., 2012. Pixel Purity Index Algorithm and n-Dimensional Visualization for ETM+ Image Analysis: A Case of District Vehari. *Global Journal of Human-Social Science Arts and Humanities*., 12(15), 76–82.

Husseinjani, M.Z., Tangestani, M.H., Velasco, F.R., Yusta, I., 2013. Sub-pixel mineral mapping of a porphyry copper belt using EO-1 Hyperion data. *Advances in Space Research*., https://doi.org/10.1016/j.asr.2013.09.004.

Singh, K., Rajaprian, K., Vinothkumar, M., Kumar, R.S., 2013. Hyperspectral remote sensing approach for lithological discrimination by ASTER data – A case study of Thenkalmalai and Odhimalai Hills, Tamil Nadu, India. *International Journal of Advanced Earth Science and Engineering*., 2(1), 75–79.

Congalton, R.G., 1991. A review of assessing the accuracy of classifications of remotely sensed data. *Remote Sensing of Environment*., 37, 35–46. https://doi.org/10.1016/0034-4257(91)90048-B.

Boardman, J.W., 1998. Leveraging the high dimensionality of AVIRIS data for improved sub-pixel target unmixing and rejection of false positives: Mixture tuned matched filtering. *Summary of the 7th Annual JPL Airborne Geoscience Workshop*., Pasadena, CA, 55.

Research Systems Inc., 2003. ENVI tutorial, ENVI software package version 4.0.

Kruse, F.A., Lefkoff, A.B., Boardman, J.W., Heidebrecht, K.B., Shapiro, A.T., Barloon, P.J., Goetz, A.F.H., 1993. The spectral image processing system (SIPS)—interactive visualization and analysis of imaging spectrometer data. *Remote Sensing of Environment*., 44(2–3), 145–163. https://doi.org/10.1016/0034-4257(93)90013-N.